ELSEVIER

Geoderma 106 (2002) 137–159

GEODERMA

www.elsevier.com/locate/geoderma

Physicochemical properties of a solonetzic toposequence

T. Toth [a], G. Jozefaciuk [b,*]

[a] *Research Institute for Soil Science and Agrochemistry of the Hungarian Academy of Sciences, Herman Otto 15 str., Budapest, Hungary*

[b] *Institute of Agrophysics of Polish Academy of Sciences, Ulica Doswiadczalna 4 str., 20-236 Lublin, Poland*

Received 5 January 2001; received in revised form 25 June 2001; accepted 16 July 2001

Abstract

Surface, charge, and pore properties of three profiles of a solonetzic toposequence: Mollic Solonetz (top), Salic Solonetz (in-between), and Haplic Solonetz (bottom) were studied. A trial of finding relations between the above and other chemical and physical parameters characterizing salt-affected soils was undertaken.

Physicochemical soil properties differed among the studied profiles and horizons. Upper, eluvial A horizons differed to the greatest extent among the profiles studied and the lowest C horizons appeared to be most similar. Surface and pore characteristics were mostly governed by organic matter and clay content. Organic matter and clay fraction increased soil surface area and amount of variable charge. The surface area increased also with amount of exchangeable bases and the CEC of the soils. Sodicity and alkalinity, mainly exchangeable sodium percentage and less the pH, appeared to reduce mesopore radii and pore complexity (fractal dimensions). © 2002 Elsevier Science B.V. All rights reserved.

Keywords: Surface area; Charge; Adsorption energy; Fractal dimension; Porosity; Solonetzic soils; Toposequence

1. Introduction

Complex geometry and chemical composition are the main reasons why surfaces of soil adsorbents are highly inhomogeneous (Sokolowska, 1989). The unique characteristic of such surfaces is provided by the adsorption energy distribution function showing fractions of surface sites of different adsorption

* Corresponding author. Fax: +48-81-7445067.
E-mail address: jozefaci@demeter.ipan.lublin.pl (G. Jozefaciuk).

0016-7061/02/$ - see front matter © 2002 Elsevier Science B.V. All rights reserved.
PII: S0016-7061(01)00122-7

energies, while the overall amount of the adsorbent surface is characterized by its surface area (Oscik, 1979). Complex structure and granular composition of the solid phase results in heterogeneity of soil pore system. A characteristic of that is provided by pore size distribution functions showing fractions of pores of different dimensions, while the overall amount of the pores is characterized by bulk and particle density or pore volume of the material (Roquerol et al., 1994). The geometrical shape of pores and surfaces may be self-similar at different scales of magnification, which can be characterized by the fractal dimension (Avnir et al., 1985; Neimark, 1990; Pfeifer and Obert, 1989). Natural objects display the fractal behavior in the limited range of scales (Pachepsky et al., 1995a). Various soil components carry electric charge of different origin, which determines the ions adsorption, pH buffering, electrostatic repulsion between charged particles, etc. (Bolt and Bruggenwert, 1976). An important part of this charge comes from dissociation of surface functional groups of different acidic strengths, which can be characterized by distribution function of surface dissociation constants (Van Riemsdijk et al., 1987).

Surface, charge, and pore properties are highly sensitive to soil chemical and mineralogical composition and location in the profile (Sokolowska et al., 1995), as well as to various processes occurring in soils such as compaction, organic matter leaching and oxidation, pH changes, silica accumulation, and/or wetting–drying cycles (Jozefaciuk et al., 1993, 1996; Lipiec et al., 1998; Pachepsky et al., 1995a,b; Wilczynski et al., 1993).

Salt accumulation in solonetzic soils is mainly determined by soil physical conditions. Large swelling and particle dispersion result in high water retention and very low hydraulic conductivity. The soils are waterlogging, sticky, and very difficult to cultivate. Although solonetzic soils share several common features, substantial vertical and lateral variations are observed. The vertical variations result from the combination of salt accumulation and leaching which produce an eluvial horizon upon the columnar–prismatic Natric B horizon. Lateral differences are often caused by different positions of the profiles on the toposequence. The above differences are expected to affect the physicochemical properties of the soil material as well as their profile distribution. The objective of this paper is to describe the physicochemical characteristics of three profiles in a toposequence of solonetzic soils and elucidate changes in these properties as affected by factors of soil formation.

2. Materials and methods

2.1. Study site

Three profiles of a solonetzic toposequence: Mollic Solonetz (MS), Salic Solonetz (SS), and Haplic Solonetz (HS) were studied. The position in the

Table 1
General characteristics of the studied solonetzic soils from Hortobagy region (Hungary)

(A) Location and soil type

Soil	Latitude N	Longitude E	Elevation (m)	D_g^a	EC_g^a	EC[a]	SAR[a]	pH[a]
MS	47°33.777′	21°18.258′	89.35	1.05	3.6	2.2	30	7.7
SS	47°33.821′	21°18.269′	89.09	0.93	6.0	6.7	85	7.9
HS	47°33.780′	21°18.170′	88.84	0.75	18.0	3.8	39	7.6

(B) Field properties

Soil	Horizon	Depth (cm)	Wet colour	Texture	Structure
MS	A	0–25	10YR 2/2	L	s-SAB
	B	25–45	10YR 2/1	CL	COL
	BC	45–68	2.5 Y 6/2	L	l-SAB
	C	> 68	2.5 Y 6/4	L	s-SAB
SS	A	0–11	10YR 4.5/2	L	s-SAB
	B	11–40	10YR 3/1	CL	COL
	BC	40–55	2.5 Y 5/4	L	SAB
	C	> 55	2.5 Y 6.5/6	L	s-SAB
HS	A	0–15	10YR 3.5/2	L	SAB
	B	15–52	10YR 2/1	CL	COL
	BC	52–68	2.5 Y 3/2	L	l-SAB
	C	> 68	2.5 Y 5/5	L	s-SAB

Abbreviations: D_g (m): groundwater depth, EC_g (mS cm^{-1}): electric conductivity of the groundwater, EC: electric conductivity, SAR: sodium adsorption ratio, and pH of soil saturation extracts from 0- to 10- and 50- to 60-cm layers.
Abbreviations: L: loam, CL: clay loam, B: blocky, SAB: subangular blocky, COL: columnar, l-: large, s-: small.
[a]Average values measured monthly in Jun–Sept 1999.

toposequence is closely related to the vegetation: grassland at the top (MS), shortgrass in-between (SS), and meadow in the bottom (HS) (Toth and Rajkai, 1994). The profiles represent a complex heterogeneous solonetzic landscape in which a difference of a few decimeters of elevation results in radically different pattern of salt accumulation. The SS profile is the most sodic and saline of the three. Basing on field observations and measurements of saturated hydraulic conductivity and surface temperature values of these profiles during a 6-year period, the following processes seem to have the most dominant effect on salt accumulation:

Profile	Processes				
	W	R	I/L	Cr	Ha
MS	−	−	+ + +	+	+ + +
SS	+	+ +	+	+ + +	+
HS	+ + +	−	+ +	+ +	+ +

The letters denote: W—waterlogging, R—runoff, I/L—infiltration/leaching, Cr—capillary rise, Ha—humus accumulation. The minus sign stands for negligible effect and the plus for positive.

The C horizon of MS profile is least affected by the above processes thus mostly resembles the original soil parent material: mixture of river and eolian sediments. Basic properties of the studied profiles are presented in Tables 1 and 2.

The field site, in the Hortobagy region of Hungary inside a 300×600-m natural pasture area, is described in more details by Toth and Kertesz (1996) and Toth and Kuti (1999a,b). Before one and a half century, the flat area of Hortobagy has been an uncontrolled watershed of the nearby Tisza river, flooding the area two to three times yearly. More recently, the effect of waterlogging consecutively decreases; however, this is still important due to fast snowmelt and heavy rainfalls and a low hydraulic conductivity of the B horizon. Hortobagy is a recharge area of the saline groundwater seeping underground from northern mountains and being a source of salt accumulation. The direction of groundwater flow changes seasonally. During the dry season, it flows downwards. During the wet season, waterlogging causes a rise in the groundwater level and a consequent flow towards the more elevated zone of SS profile, similarly as described by Seelig and Richardson (1994) for salt-affected North Dakota soils.

Table 2
Laboratory characteristics of the studied solonetzic soils

Soil and horizon		CO_3^{2-} (%)	OM (%)	CEC	EB	ESP (%)	pH	EC	SAR	BD	Ks	Silt (%)	Clay (%)
MS	A	0.25	4.22	25.0	15.5	3.04	8.15	0.89	4.5	1.19	81.7	67.1	15.7
	B	0.38	2.06	17.4	20.7	83	8.68	0.75	98.1	1.42	0.014	54.4	43.8
	BC	20	0.93	18.5	13.0	82.8	9.07	6	106.8	1.55	0.023	60.2	42.9
	C	32.3	0.53	10.9	10.9	93.5	9.18	5.4	96.2	1.64	0.012	65.6	33.4
SS	A	0.17	1.56	15.2	8.7	74.9	8.53	10.3	125.6	1.46	0.028	80.1	28.8
	B	0.59	0.88	20.7	21.1	92.9	9.05	9.3	222.6	1.56	0.144	54.4	42.1
	BC	25.2	0.54	13.0	16.9	95.8	9.31	11	271.2	1.66	0.161	59.0	36.1
	C	16.8	0.27	10.9	11.7	81.8	9.25	5.8	160.2	1.64	0.119	63.3	27.2
HS	A	0.08	4.08	10.9	16.1	10	7.8	0.75	13.8	1.18	8.80	79.7	14.2
	B	0.08	1.38	21.7	17.4	60.9	8.26	6.7	76.6	1.62	0.006	54.5	42.7
	BC	0.5	0.66	17.4	18.6	64.4	8.2	8.7	81.3	1.61	0.010	53.4	36.1
	C	19.3	0.37	12.0	10.9	72.5	8.18	10.5	79.3	1.62	0.143	60.6	26.7

Abbreviations: CO_3^{2-}: carbonates content, OM: organic matter content, CEC and EB (exchangeable bases): cmol kg^{-1}, ESP: exchangeable sodium percentage, SAR: sodium adsorption ratio, BD: bulk density, Ks: saturated hydraulic conductivity (cm/day), EC: electric conductivity (mS cm^{-1}); Ks, EC, pH, and SAR were determined in the saturation extract.

3. Methods of soil analysis

3.1. Surface area and energy characteristics

Water vapor adsorption isotherms were measured using vacuum chamber method at a temperature $T = 294 \pm 0.1$ K. To reach different relative water vapor pressures, p/p_0, ranging from ca. 0.001 to 0.99, sulfuric acid of stepwise decreasing concentrations was used. The amount of adsorbed water at a given p/p_0 was measured after 48 h of equilibration by weighing. The dry mass of the samples was estimated after 24 h of oven drying at 378 K after the completion of the isotherm measurements. For mathematical description of adsorption data, the Aranovich (1992) isotherm was used, which in linear form reads:

$$x\Big/\left[a(1-x)^{1/2}\right] = 1/(a_{\mathrm{m}}C) + x/a_{\mathrm{m}}, \tag{1}$$

where $x = p/p_0$, a (kg kg^{-1}) is the amount adsorbed, a_{m} (kg kg^{-1}) is the statistical monolayer capacity, and $C = \exp(E_{\mathrm{a}} - E_{\mathrm{c}})/RT$ is the constant related to the adsorption energy, E_{a} (J mol^{-1}), and the condensation energy of water, E_{c} (J mol^{-1}). Contrary to the standard Brunauer–Emmett–Teller (BET) isotherm, the Aranovich isotherm permits the presence of vacancies in the adsorbed layer and is thermodynamically correct. This isotherm equation fits the experimental polymolecular adsorption data within a broader range of relative pressures than the BET does, and is applicable to data on water vapor adsorption on soils (Jozefaciuk and Shin, 1996a).

The surface area values, S, were calculated as:

$$S = N_{\mathrm{A}}\,\omega\, a_{\mathrm{m}} M^{-1}, \tag{2}$$

where N_{A} is Avogadro's number, M (kg) is molecular mass of water, and $\omega = 1.08 \times 10^{-19}$ m^2 is the area occupied by a single water molecule.

Using a theory of adsorption on heterogeneous surfaces (Jaroniec and Brauer, 1986; Jaroniec et al., 1975) and applying the Aranovich isotherm to describe local adsorption effects and the condensation approximation (Harris, 1968), the adsorption energy distribution functions showing fractions of surface sites of various adsorption energies, $f(E_i)$, were calculated from adsorption data as:

$$f(E_i) = \left[(1-x_{i+1})^{1/2}\Theta(E_{i+1}) - (1-x_i)^{1/2}\Theta(E_i)\right]\Big/(E_{i+1} - E_i), \tag{3}$$

where $E_i = (E_{\mathrm{a},i} - E_{\mathrm{c}})$, $E_{\mathrm{a},i}$ is the adsorption energy of the i-th site, and $\Theta(p) = a(p)/a_{\mathrm{m}}$ is the adsorption isotherm. For calculations, the dimensionless adsorption energies, E_i/RT, were used. To convert these dimensionless values to the SI units, one uses the following dependence:

$$E\,(\mathrm{kJ\,mol^{-1}}) = -44 + 2.48\,E/RT,$$

where -44 kJ mol^{-1} is the condensation energy of water vapor and 2.48 kJ mol^{-1} $= RT$ for $T = 298$ K. The dimensionless energy range from -9 to 0 was

considered. The value of 0 corresponds to the adsorption energy equal to the condensation energy of water vapor, and the value of -9 was assumed to be the maximum adsorption energy value for the whole adsorbent. The E_i/RT range considered was divided into subranges of 1 E_i/RT unit. The values of Θ for the end values of each subrange were estimated by linear interpolation of the nearest data points.

The average water vapor adsorption energy, E_{av}, was calculated from $f(E_i)$ values as:

$$E_{av} = \sum_{i=1}^{n} E_i f(E_i). \tag{4}$$

Details on the above experimental method and calculations can be found in Jozefaciuk and Shin (1996a,b).

3.2. Micropore characteristics

Water vapor desorption isotherms were measured using the vacuum chamber method as described above, but sulfuric acid of stepwise increasing concentrations (decrease of p/p_0) was used. Characteristics of pores ranging from ca. 1 to a few tens of nanometers were evaluated from desorption values. These pores are later called micropores. The average micropore radius, r_{av} was obtained as:

$$r_{av} = 1/(2\upsilon_t)\sum_{i=1}^{n}(r_i + r_{i+1})\big(\upsilon(r_{i+1}) - \upsilon(r_i)\big) \tag{5}$$

and fractions of pores in the given range of radii, $f(r_{av,i})$ as:

$$f(r_{av,i}) = \big(\upsilon(r_{i+1}) - \upsilon(r_i)\big)/\upsilon_t. \tag{6}$$

The assumptions have been made that the radius of the micropore, r, in the capillary condensation process is related to the vapor pressure p by the Kelvin equation for the hemispherical meniscus with zero water/solid contact angle, and that the condensation in micropores occurs above $p/p_0 = 0.35$. Thus, the total micropore volume, υ_t, was taken as the volume of adsorbed water at the maximum p/p_0 value applied minus that at $p/p_0 = 0.35$. Details on the above calculations can be found in Jozefaciuk et al. (1999). The total range of mesopore radii was divided on three subranges equal to each other in logarithmic scale, and the $f(r_{av,i})$ value was determined for each subrange. The values of $\upsilon(r_{i+1})$ and $\upsilon(r_i)$ for the above calculations were taken from linear interpolation of experimental data for the end values of every subrange.

From desorption data, the fractal dimensions, D, were calculated using the Avnir and Jaroniec equation (Jaroniec and Kruk, 1997):

$$\ln(a) = \text{constant} + (D-3)\ln\big(RT\ln(p_0/p)\big). \tag{7}$$

3.3. Mesopore characteristics

Mercury intrusion porosimetry (MIP) measurements were performed for natural soil aggregates. Before the measurements, the aggregates were subjected to a few wetting–drying cycles to stabilize the structure and crushed into 3- to 4-mm (diameter) pieces. The MIP curves relating the intruded volume of mercury, V, to the mesopore radius, R, were used to evaluate average mesopore radii, size distribution functions (Sridharan and Venkatappa Rao, 1972), and fractal dimension of mesopore surface, D_s. The two former characteristics were calculated in the same way as described previously for micropores. However, having much more experimental points, the total range of mesopore radii was divided on (logarithmic) subranges equal to 0,1. The mesopore surface fractal dimension was evaluated from the slopes of the linear parts of the log–log plots of the equation (Pachepsky et al., 1995a):

$$\mathrm{d}V(R)/\mathrm{d}R \propto R^{2-D_s} \tag{8}$$

from the following dependence:

$$D_s = 2 - \text{slope} = 2 - \mathrm{dlog}\left[\mathrm{d}V(R)/\mathrm{d}R\right)\right]/\mathrm{dlog}\,R. \tag{9}$$

3.4. Variable surface charge characteristics

The back titration procedure (Duquette and Hendershot, 1993), modified to avoid exchangeable acidity and high dilution effects (Jozefaciuk and Shin, 1996c), was used to evaluate variable surface charge vs. pH dependencies. Before the titration, carbonates were removed from the samples by pH 3 HCl treatment. The amount of surface charge was found as the amount of base consumed by the suspension minus that consumed by the equilibrium solution. Variable charge equal to zero was assumed for the beginning of titration. The maximum charge measured within the experimental pH range (e.g. between pH = 3 and 9) was taken as the total amount of the variable charge, Q^-. From variable charge vs. pH curves, the distribution functions of apparent surface dissociation constants, K_{app}, (Van Riemsdijk et al., 1987) were calculated:

$$f(\mathrm{p}K_{\mathrm{app},i}) = 1/Q^-\left[\Delta Q^-(\mathrm{pH}_{i+1}) - \Delta Q^-(\mathrm{pH}_i)\right]/(\mathrm{p}K_{\mathrm{app},i+1} - \mathrm{p}K_{\mathrm{app},i});$$

$$\mathrm{p}K_{\mathrm{app}} = \mathrm{pH}, \tag{10}$$

where $\mathrm{p} = -\log$, $f(\mathrm{p}K_{\mathrm{app},i})$ denotes the fraction of surface sites of i type and having dissociation constants equal to $K_{\mathrm{app},i}$, and $\Delta Q^-(\mathrm{pH})$ is the variable surface charge increase with increase of pH.

Knowing the apparent surface dissociation constants distribution functions, the average pK_{app} values were determined:

$$pK_{app,av} = \sum_{i=1}^{n} pK_{app,i} f_i(pK_{app}). \quad (11)$$

Details on these calculations are given in Jozefaciuk and Shin (1996d).

Final results of all the calculations described above were obtained by averaging over three independent measurements.

3.5. Field methods and routine laboratory analysis

Soil profiles were described in field and analyzed in laboratory using methods presented by Buzás (1988).

4. Results and discussion

4.1. Isotherms and adsorption energy

Water vapor desorption curves of the studied soils are presented in Fig. 1. Adsorption branches are not included in the figure to have clearer drawings. Adsorption–desorption hysteresis loops for all samples were not large and started about $p/p_0 = 0.3$–0.4. In general, the highest water vapor adsorption occurs in B horizons. Relatively high adsorption is observed also for the BC horizon of MS profile.

Adsorption energy distribution functions (Fig. 2) calculated from adsorption branches (Eq. (3)) have similar shapes for each horizon of SS soil. This profile is most homogeneous with respect to surface energetic properties. Large salinity, sodicity, and pH coupled with low hydraulic conductivity resulting in high surface runoff, low biotic activity, and low level of humus accumulation could highly homogenize the SS profile material. Adsorption energy patterns for deeper horizons of MS and HS profiles are very similar to those of the SS profile, which indicates that the study area contains soil material of rather homogeneous surface properties.

Energy distribution functions for eluvial A horizons of HS and MS profiles differ from those of the lower horizons. Fractions of low-energy adsorption centers are smaller, and high-energy centers are greater than in deeper horizons. High-energy centers in A horizons can arise from high amount of polar, hydrophilic groups on organic surfaces. The energy distribution function of organic matter of “normal” soils is skewed in the direction of lower energies as can be concluded from Sokolowska et al. (1993, 1995), which reflects high amounts of less polar or apolar groups. Indeed, the fulvic character and greater solubility of organic matter in saline soils indicate that it has a more polar

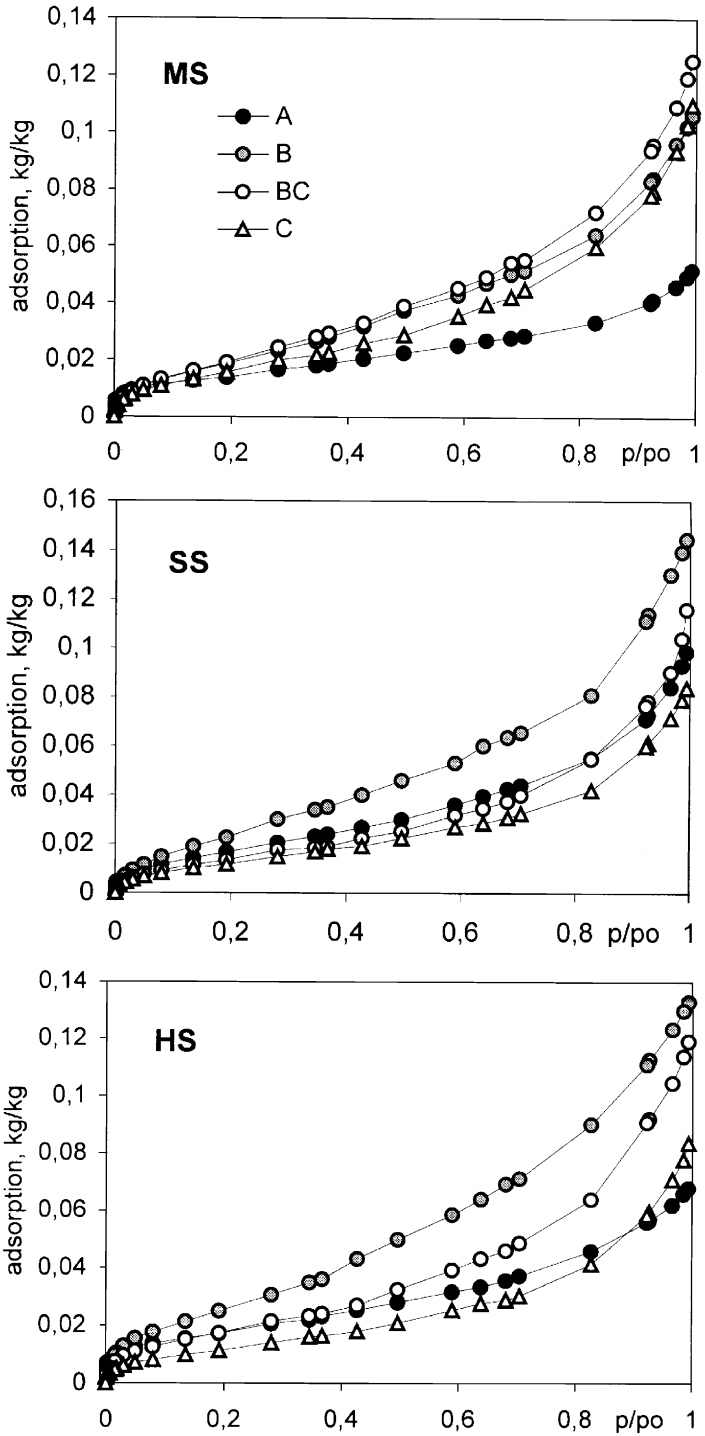

Fig. 1. Water vapor desorption isotherms for the studied samples.

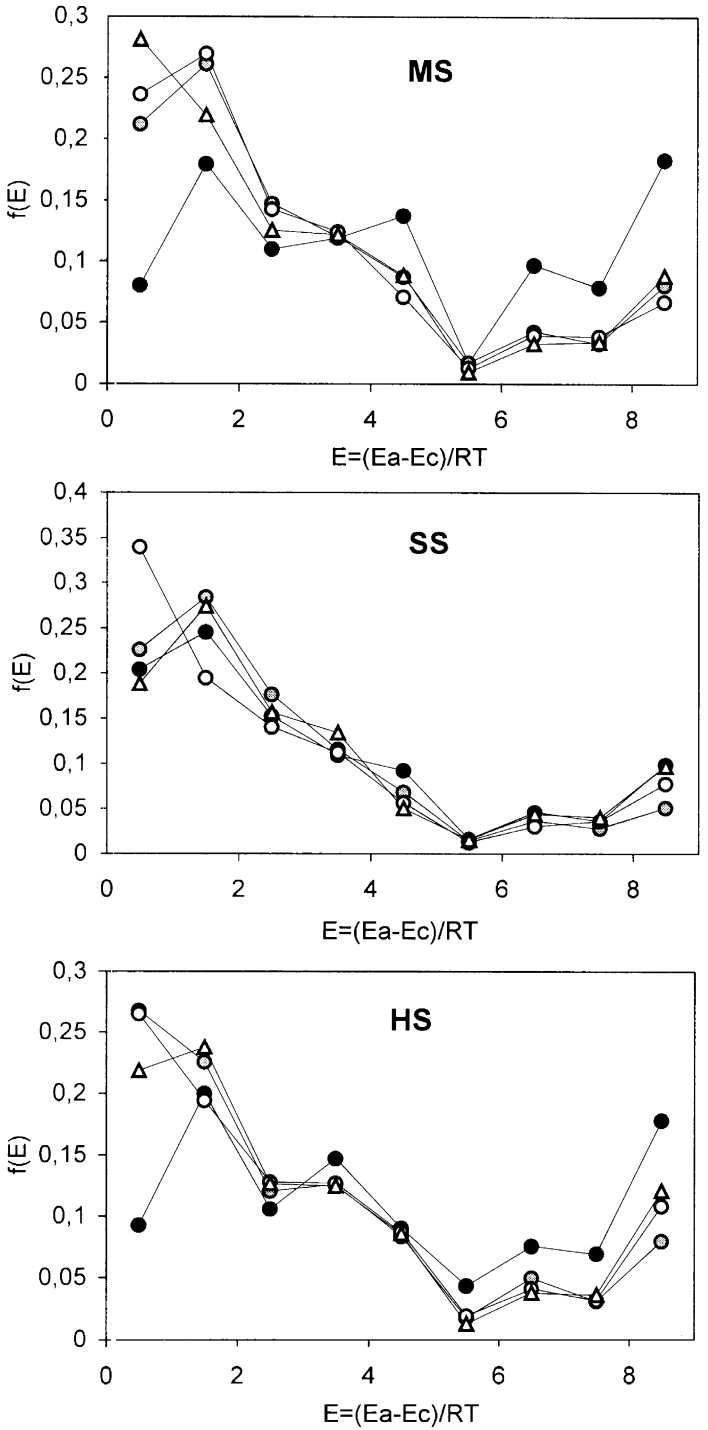
MS
SS
HS
f(E)
E=(Ea-Ec)/RT
0
0,05
0,1
0,15
0,2
0,25
0,3
0,35
0,4
2
4
6
8

character than humic organic matter in "normal" soils. Also, higher amount of low-energy centers in deeper profiles, except lower amount of OM, can be due to the effect of salinity, that is, the increase of exchange sodium ions. Monovalent sodium cations bind water with lower energy than the divalent ones such as Ca and Mg.

4.2. Microporosity

Micropore size distributions evaluated from desorption isotherms are presented in Fig. 3. Fractions of the largest micropores are lowest in all horizons. Usually the smallest micropores dominate; however, the medium-sized micropores dominate in deeper horizons of SS and HS profiles. The micropores of the studied soils seem to be fractal what is seen from the linearity of ln–ln plots of adsorption vs. adsorption potential (fractal plots). An example is presented in Fig. 4. The fractal behavior corresponds to small micropore sizes, so this may be related to surface roughness, as well.

4.3. Mesoporosity

Mesopore size distribution functions (Fig. 5) illustrate that eluvial A horizons have the largest mesopores. The smallest pores occur usually in BC horizons. The mesopore size distribution of particular horizons in MS profile is most contrasting. For the formation of large pores in A horizons, an accumulation of structure-forming organic matter and strong biological activity can be responsible. The mesopore size distribution function for C horizons of all profiles has very similar shape. However, the peak of dominant pores is shifted towards larger sizes with decrease of elevation in the toposequence. As the MS profile is least affected by the standing water, the peak at 0.25 μm [$\log(R) = -0.6$] can be considered as typical for the parent sediment. SS and HS profiles get more water than the MS. Therefore, in these profiles, the restructuring effect of wetting and drying cycles is more pronounced. This may cause mesopore loosening, for example, the observed shift of the dominant mesopore peak in C horizons.

The mesopore surfaces of the studied soils exhibit apparently two fractality ranges for small and large mesopores which is exemplary illustrated for the MS soil (Fig. 6) showing the log–log plots of Eq. (8) together with linearity ranges corresponding to fractal pore surface behavior. The slopes of the linear fits for the large mesopore range are very high, so the corresponding fractal dimensions of the pore surfaces are much higher than 3, which has no physical meaning.

Fig. 2. Adsorption energy distribution functions for the studied samples. Abbreviations as in Fig. 1.

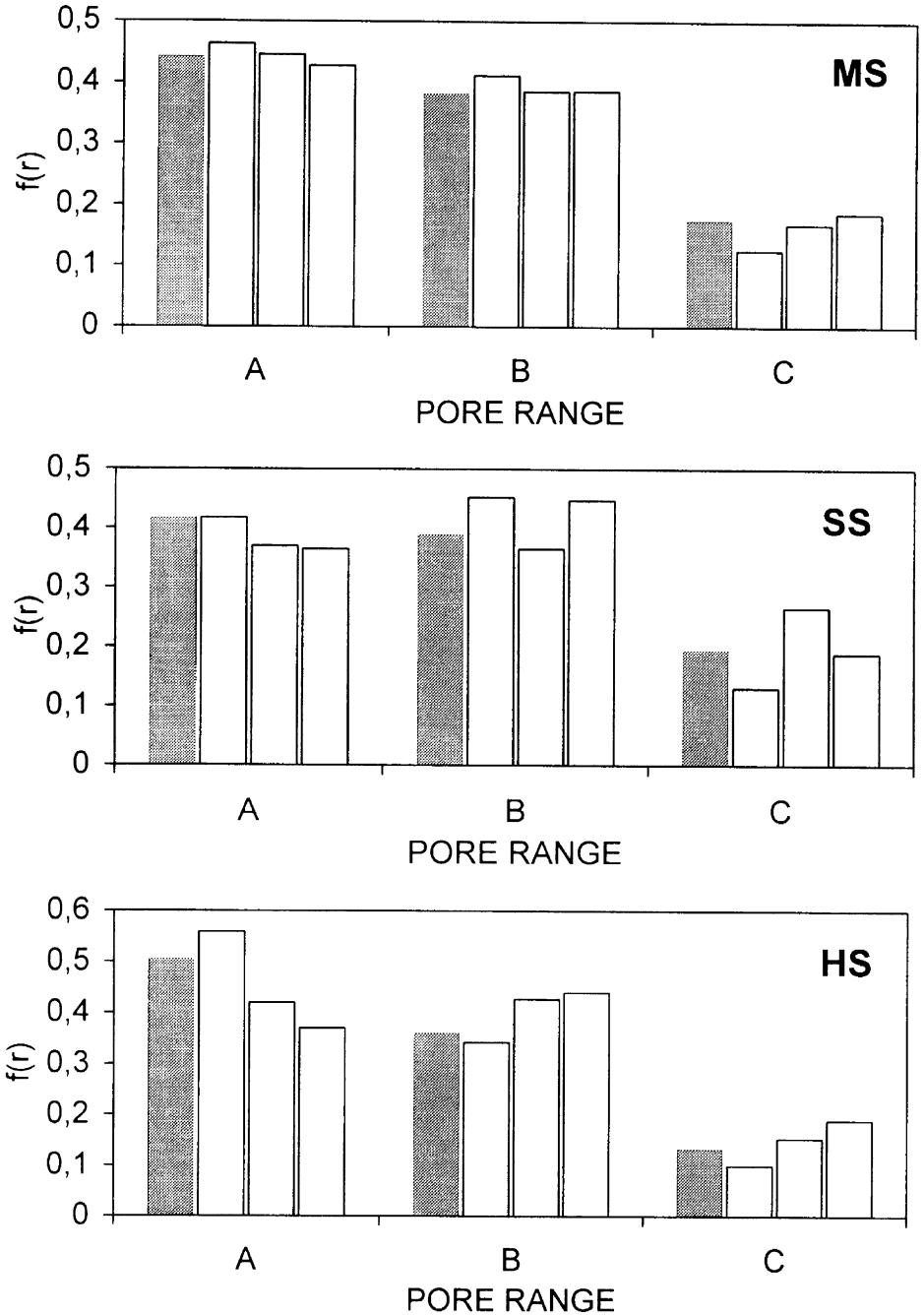

Fig. 3. Micropore size distribution functions for the studied samples. Gray bars denote the upper horizon. Next bars from the left to right denote deeper horizons, subsequently. Pore ranges: (A) 2–8 nm, (B) 8–32 nm, (C) 32–128 nm.

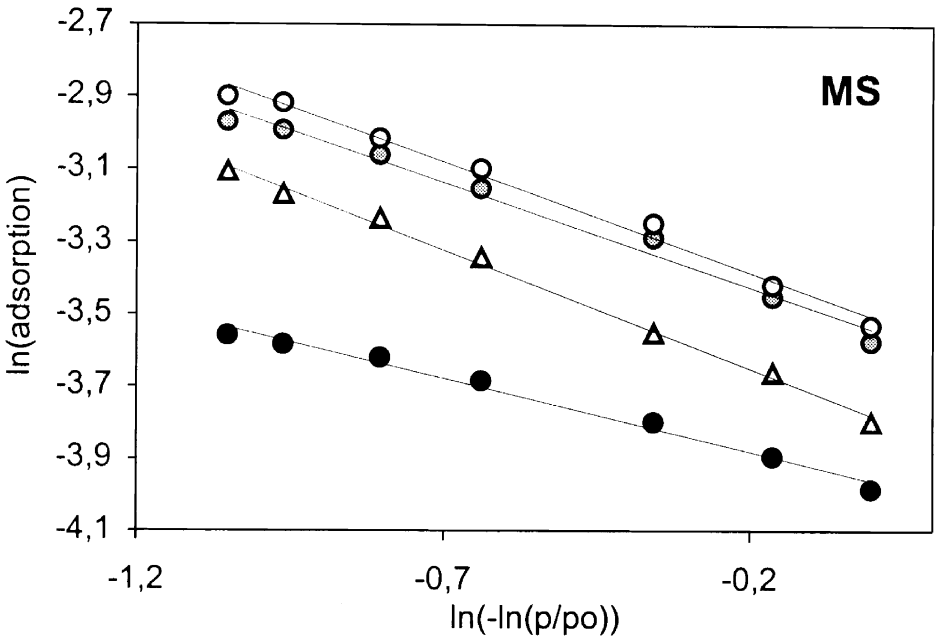

Fig. 4. Exemplary fractal plot for micropores (MS profile). Abbreviations as in Fig. 1.

Possibly in this range, pores are formed from larger voids connected by narrower necks and the volume of the void is attributed to the radius of the neck. Therefore, the pore volume is higher than formally possible to calculate maximal $D_s = 3$ in a cylindrical pore model (dV/dR is higher and leads to higher D_s). Such neck–void structures are likely to be formed by larger particles (Czachor, 1997).

4.4. Variable surface charge

The variable charge Q^- vs. pH dependencies are shown in Fig. 7. In general, the variable charge of soil horizons developed below pH ≈ 8 values decreases in the following sequence: B, A, BC, and D. Above this pH, the Q^- in eluvial A horizons of MS and HS soils starts to increase faster than those in the other horizons, which results in the highest charge in A horizons at high pH values. This indicates that soil material of these profiles contains rather high amount of weakly acidic surface functional groups.

The variable charge in soils originates mainly from soil organic matter and from clay mineral edges and amorphous Al or Fe oxides (Bolt and Bruggenwert, 1976; Uehara and Gillmann, 1981). The latter can be accumulated mainly in B horizons of the studied soils, as concluded from data on Hungarian solonetzic soils (Szendrei, 1983). Relatively high charge of A horizons comes most

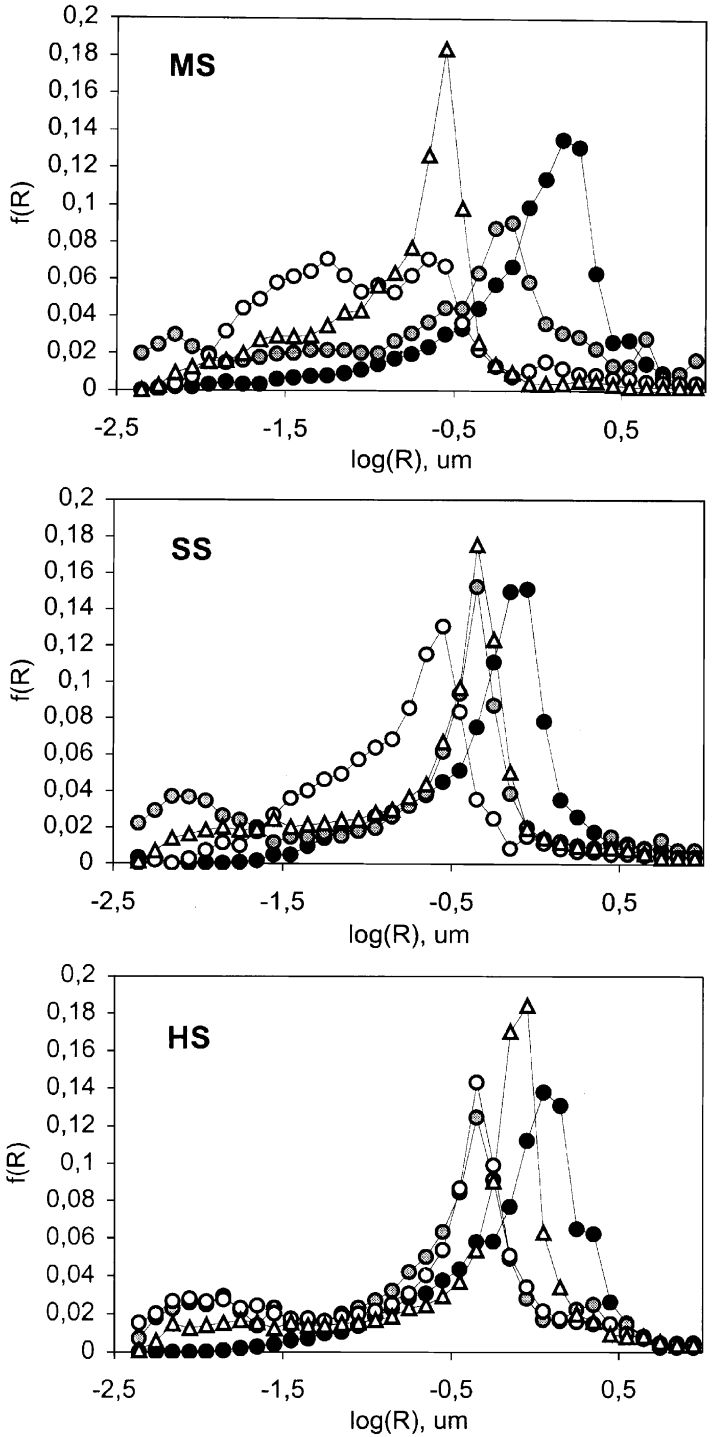

Fig. 5. Mesopore size distribution functions for the studied samples. Abbreviations as in Fig. 1.

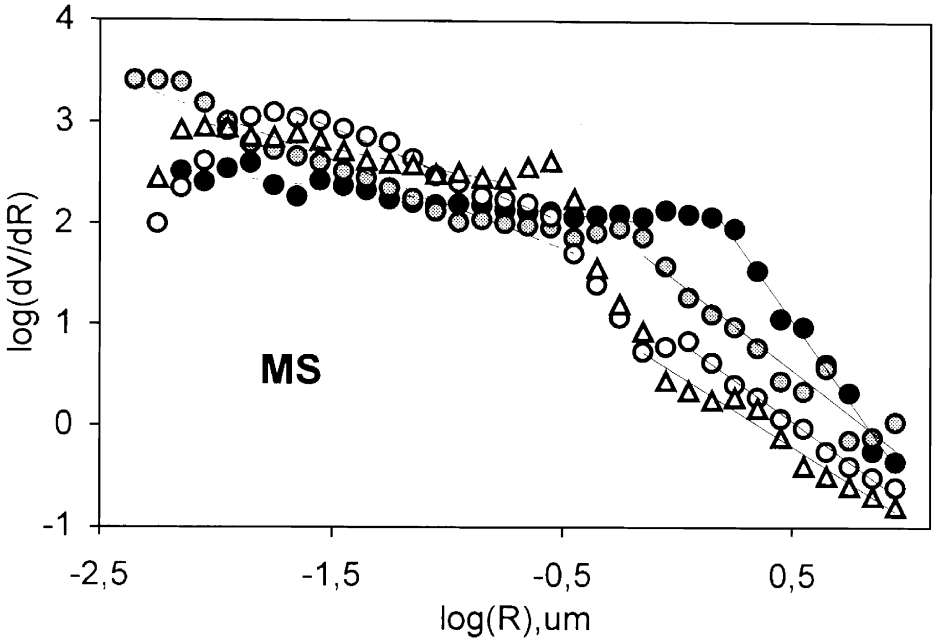

Fig. 6. Exemplary fractal plot for mesopores (MS profile) including linearity ranges of Eq. (8). Abbreviations as in Fig. 1.

probably from organic matter having the highest amount of variable charge per unit mass.

The character of variable charge can reflect processes of soil formation. The original deposits from which the soils are formed (C horizons) have the lowest amount of variable charge. In upper horizons, soil genetic processes of various kind and intensity can lead to the formation of new soil components of different charge characteristics.

Apparent surface dissociation constants (pK_{app}) distribution functions are shown in Fig. 8. The presence of rather high amounts of surface functional groups of medium acidity (a peak around $pK_{app} = 6$) is typical for the studied profiles. These groups locate most probably on amorphous Fe or Al hydroxides. The smallest amount of these components should occur in A horizons as indicated by the lowest peaks. The lowest amount of amorphous Al and Fe hydroxides in Hungarian saline soils occurs in A horizon (Szendrei, 1983). However, surfaces of Al and Fe oxides may be coated by organic components as well. In A horizons, this peak is highest for SS soil, where organic matter effect on soil properties is the weakest.

4.5. General analysis of the soil physicochemical characteristics

Surface, pore, and variable charge parameters of the studied soils are summarized in Table 3.

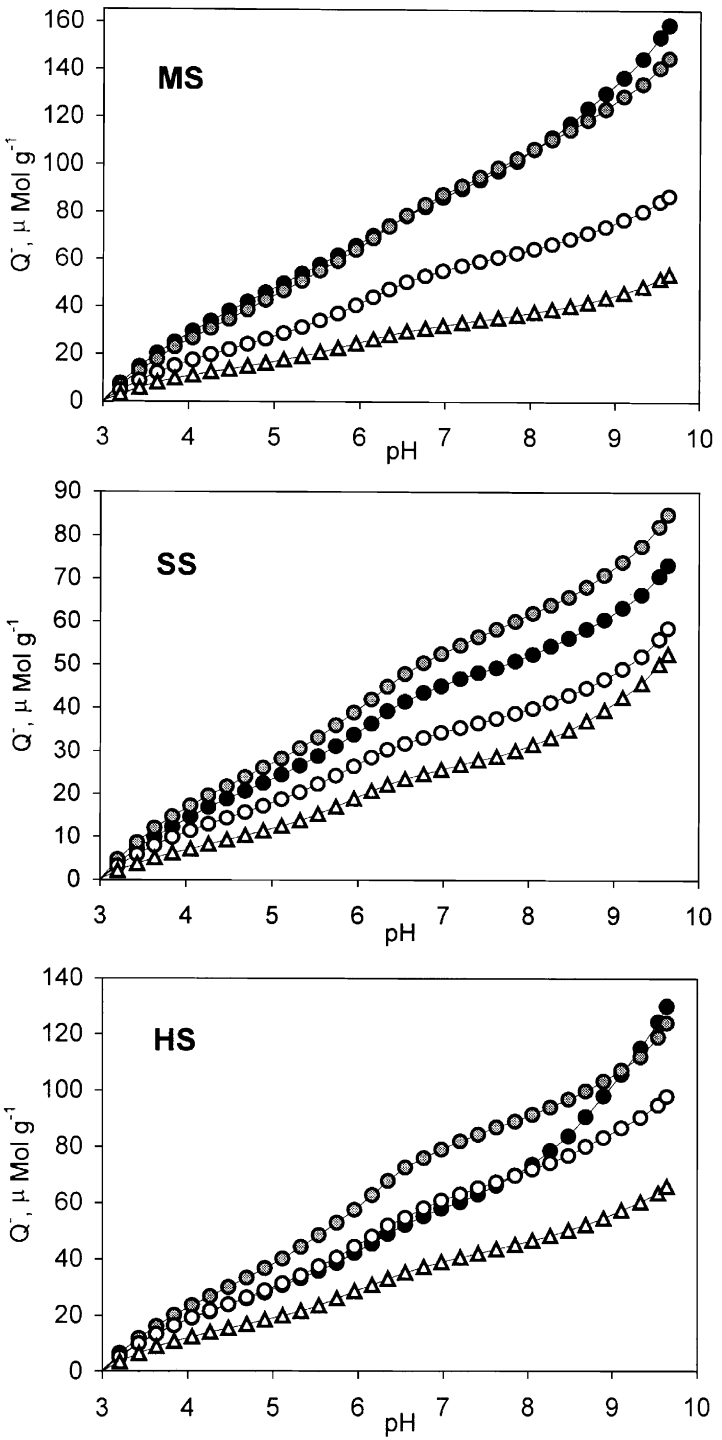
MS
SS
HS
Q⁻, μ Mol g⁻¹
pH

The average adsorption energy is significantly higher in A than in deeper horizons. This can be due, as already mentioned, to highly polar character of organic matter in saline soils, which adsorb water with high energy. The rise of salinity and sodicity (exchangeable sodium percentage and sodium adsorption ratio) with the profile depth may also decrease adsorption energy due to lower hydratation energy of sodium than the other ions, as mentioned earlier. Amorphous silica oxides which can accumulate in fine granulometric fractions of deeper horizons can lead to similar results. Despite large surface areas, such adsorbents have low water vapor adsorption energies (Gregg and Singh, 1967). Possibly similar features may have amorphous aluminum or iron oxides.

The surface area S is highest in B horizons which appears to be due to the highest clay and exchangeable basic cations EB content. Surface cations are water adsorption centers (Newman, 1985). The correlations of S and CEC or clay have been frequently reported in the literature (Petersen et al., 1996; Sokolowska, 1989). These are noted also for the studied solonetzic soils; however, the correlations are better after excluding eluvial A horizons.

The correlation between surface area and organic matter is observed for deeper horizons of the studied soils. From the slope of the S–OM regression line, one can estimate the surface area of organic matter in the studied solonetzic soils. The result is around 2800 m^2/g of organic matter. Surface area of soil organic matter in "normal" soils accounts for a few hundreds square meters per gram (Wilczynski et al., 1993). Indeed, small (fulvic) organic matter particles of high charge and polarity may have much higher surface areas than more hydrophobic, larger organic particles in "normal" soils. In upper horizons of MS and HS profiles, the surface area is lower than can be expected basing on the organic matter content. In upper horizons, properties of organic matter may be different. In deeper horizons, more mobile organic particles may be accumulated. From the other point of view, the organic material may decrease surface area of the mineral soil components by gluing smallest pores and making them unavailable for water vapor adsorption (Sokolowska et al., 1993). The maximum hygroscopicity value of the studied soils increases with the surface area. The correlation coefficient R^2 for this relationship equal to 0.93 was found.

The average micropore radii are smallest in B horizons, which may indicate that these horizons, together with the highest amount of clay, contain the finest clay particles. The volumes of micropores, increasing generally with the amount of clay fraction, are smallest in A horizons. For the MS profile, the highest micropore volumes are noted in BC and C horizons, whereas for SS and HS, these are highest in B and BC horizons.

Fig. 7. Solid phase variable charge vs. pH dependencies for the studied samples. Abbreviations as in Fig. 1.

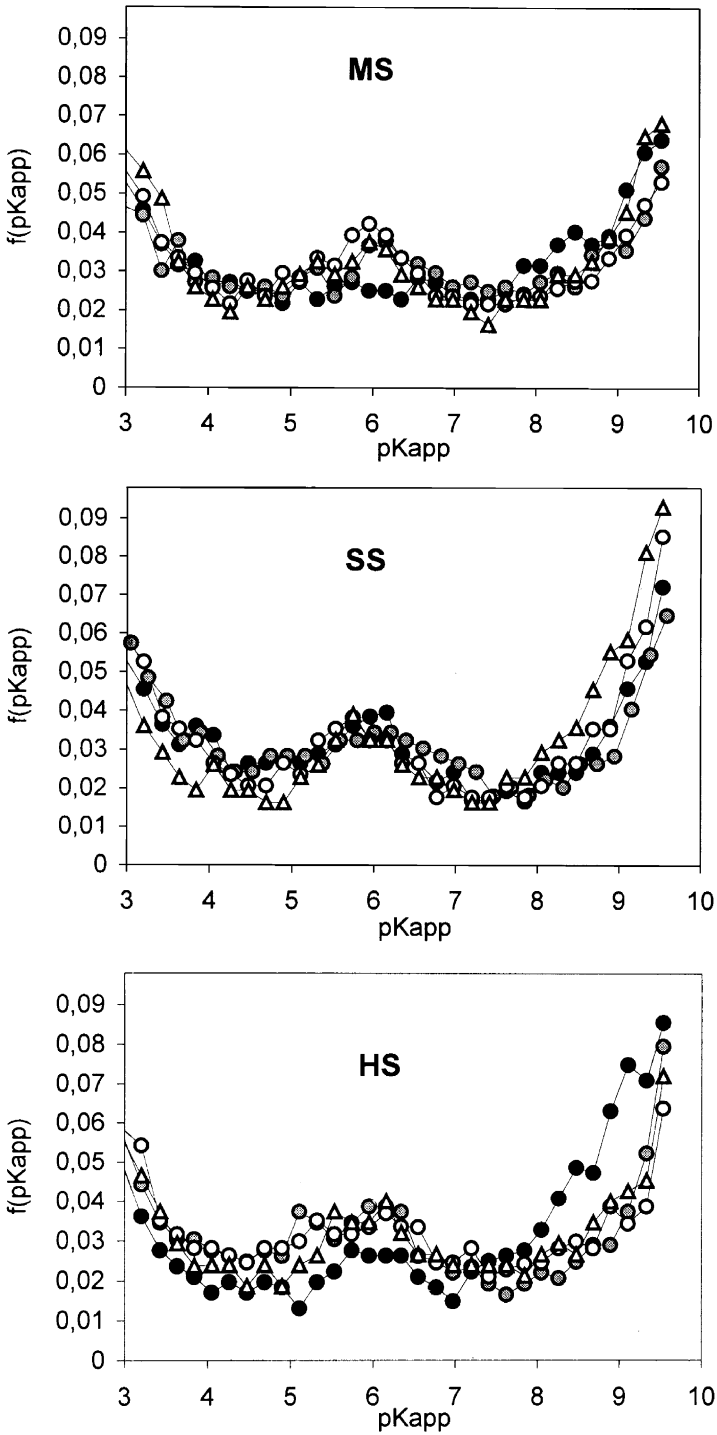
MS
SS
HS
f(pKapp)
pKapp
0,09
0,08
0,07
0,06
0,05
0,04
0,03
0,02
0,01
0
3
4
5
6
7
8
9
10

Micropore fractal dimensions D are significantly higher in A than in the deeper horizons, indicating that the surfaces (or fine micropores) of the A horizons solid material are mostly rough and complicated. This effect is the least pronounced in the SS profile, in which the amount of organic matter is the least. Surfaces in deeper horizons are smoother, closer to two-dimensional surfaces. The D value decreases with the increase of exchangeable sodium percentage.

The radii of mesopores are highest in A horizons which can reflect the highest amount of coarser material (silt fraction) and lowest bulk density controlled mainly by soil organic matter. Mesopore volumes, reflecting soil granulometric composition (as these decrease with clay and increase with silt content), are highest in A horizons of MS and HS profiles and in the C horizon of the HS. The amount and radii of mesopores can also affect saturated hydraulic conductivity values. In the C horizons, we found the MS profile to have the smallest and the HS the largest value of hydraulic conductivity. Mesopores are, at least in part, responsible for water holding capacity of the studied soils, what is concluded from positive correlations of average mesopore radii and the soil water content at $pF = 0$ value. However, rather the mesopore volume should correlate with the latter.

Smallest fractal dimensions of mesopore surface in the range of smaller pores, $D_s(S)$, occur in A horizons, whereas in these horizons, the surfaces of larger mesopores have highest fractal dimensions, $D_s(L)$. For upper horizons of the studied soils, with low carbonate content, the $D_s(S)$ value increases linearly with increase of calcium carbonate (close correlation with $R^2 = 0.95$). Here the effect of calcium ions on soil structure formation may be expressed. The $D_s(L)$ value decreases with increase of exchangeable sodium percentage and calcium carbonate content, similarly as micropore fractal dimension, D; however, the correlations with the carbonates are poor.

The amount of variable charge decreases down the profiles which is due to the decrease in both organic matter and clay content. As the variable charge results from all surfaces able to associate/dissociate protons, one may also suspect that less weathered mineral material, generating less charge, occurs in deeper horizons. The pK_{app} values in SS and HS are highest in upper horizons, whereas the opposite is true in SH. In general, the whole soil material exhibits weak acidic properties as can be concluded from high values of pK_{app}. In "normal" soils, the values of pK_{app}, calculated also from pH = 3 to 9 titration data, are from 0.3 to 1 unit lower, whereas the amount of variable charge (from data of Dabkowska-Naskret, 1988 divided by clay content for more exact comparison), is usually higher.

Fig. 8. Apparent surface dissociation constants distribution functions for the studied samples. Abbreviations as in Fig. 1.

Table 3
Surface and pore parameters of the studied solonetzic soils

Soil and horizon		E_{av}/RT	S ($m^2\ g^{-1}$)	r (nm)	v ($mm^3\ g^{-1}$)	D	Q^- ($\mu mol\ g^{-1}$)	pK_{app}	R (μm)	V ($mm^3\ g^{-1}$)	$D_s(S)$	$D_s(L)$
MS	A	4.29	73	16.9	34	2.50	159	6.53	1.27	288	2.25	5.21
	B	2.91	141	14.0	79	2.22	145	6.34	0.91	136	2.86	3.76
	BC	3.10	96	19.2	97	2.18	87	6.24	0.36	116	3.49	3.51
	C	3.21	62	23.8	88	2.23	54	6.37	0.30	148	2.44	3.42
SS	A	3.15	87	22.7	75	2.26	73	6.31	0.89	122	2.31	4.28
	B	2.65	130	18.0	111	2.13	85	6.29	0.63	132	3.32	3.62
	BC	2.66	82	29.4	98	2.17	59	6.43	0.39	123	2.44	3.65
	C	3.09	64	23.0	67	2.22	53	6.89	0.51	142	2.75	3.90
HS	A	4.48	58	21.5	46	2.45	130	6.99	1.09	273	2.14	5.35
	B	2.98	102	17.4	98	2.22	124	6.28	0.62	96	2.12	3.95
	BC	2.81	110	20.5	96	2.26	98	6.30	0.57	160	3.17	4.01
	C	2.87	89	22.8	68	2.27	66	6.42	0.78	210	2.81	4.29

Abbreviations: E_{av}/RT: average adsorption energy, S: surface area, r: average mesopore radius, v: mesopore volume, D: micropore fractal dimension, Q^-: variable surface charge, pK_{app}: apparent surface dissociation constant, R: average mesopore radius, V: mesopore volume, $D_s(S)$ and $D_s(L)$: fractal dimension of smaller and larger mesopore surface, respectively (see text).

5. Conclusions

Surface and pore properties of the studied solonetzic soils differ significantly in depth of the profile and vary with the location in toposequence. The profile located on the top of the studied area and in the bottom have more similar properties as compared to this in-between.

Surface, pore, and charge properties developed during formation of Solonetz profiles seem to depend on a very complex set of soil physical and chemical variables, which in turn are governed by environmental influences. Among these variables, as this is observed in nonsaline soils, organic matter and granulometric composition play the most important role. Exchangeable sodium percentage showed significant effect on soil pore build-up.

To better describe the physicochemical basis of the processes leading to profile differentiation in solonetzic landscapes and their consequences on surface and pore properties, more research is needed, including especially a greater variety of salt-affected soils. We plan to make such experiments in the near future.

Acknowledgements

Research and publication was supported by the EU Program no. PL970598, contract no. ENV4-CT97-0681, the Hungarian-Polish Academic Bilateral Exchange program and the Hungarian Scientific Fund Projects nos. T 023271 and T 030738.

References

Aranovich, G.L., 1992. The theory of polymolecular adsorption. Langmuir 8, 736–739.

Avnir, D., Farin, D., Pfeifer, P., 1985. Surface geometric irregularity of particulate materials: the fractal approach. J. Colloid Interface Sci. 103, 112–123.

Bolt, G.H., Bruggenwert, M.G.M., 1976. Soil Chemistry: A. Basic Elements. Elsevier, Amsterdam.

Buzás, I. (Ed.), Methods of Soil Analysis. Mezőgazdasági Kiado, Budapest (in Hungarian).

Czachor, H., 1997. Solid phase geometry and pore space in agricultural granular materials on example of mineral soil. Acta Agrophys. 7, 1–80.

Dabkowska-Naskret, H., 1988. Characteristics of surface charge of selected soils. Soil Sci. Annu. T. XXXIX 3, 223–227 (in Polish).

Duquette, M., Hendershot, W., 1993. Soil surface charge evaluation by back-titration: I. Theory and method development. Soil Sci. Soc. Am. J. 57, 1222–1228.

Gregg, S.J., Singh, K.S., 1967. Adsorption, Surface Area and Porosity. Academic Press, London.

Harris, L.B., 1968. Adsorption on a patchwise heterogeneous surface: I. Mathematical analysis of the step-function approximation of the local isotherm. Surf. Sci. 10, 129–145.

Jaroniec, M., Brauer, P., 1986. Recent progress in determination of energetic heterogeneity of solids from adsorption data. Surf. Sci. Rep. 6, 65–117.

Jaroniec, M., Kruk, M., 1997. Fractal analysis of composite adsorption isotherms by using density functional theory data for argon in slitlike pores. Langmuir 13, 1031–1035.

Jaroniec, M., Rudzinski, W., Sokolowski, S., Smarzewski, R., 1975. Determination of energy distribution function from observed adsorption isotherms. J. Colloid Polym. Sci. 253, 164–166.

Jozefaciuk, G., Shin, J.S., 1996a. Water vapor adsorption on soils: I. Surface areas and adsorption energies as calculated by the BET and a new Aranovich theories. Korean J. Soil Sci. Fert. 29, 86–91.

Jozefaciuk, G., Shin, J.S., 1996b. Water vapor adsorption on soils: II. Estimation of adsorption energy distributions using local BET and Aranovich isotherms. Korean J. Soil Sci. Fert. 29, 218–225.

Jozefaciuk, G., Shin, J.S., 1996c. A modified back-titration method to measure soil titration curves minimizing soil acidity and dilution effects. Korean J. Soil Sci. Fert. 29, 321–327.

Jozefaciuk, G., Shin, J.S., 1996d. Distribution of apparent surface dissociation constants of some Korean soils as determined from back titration curves. Korean J. Soil Sci. Fert. 29, 328–335.

Jozefaciuk, G., Sokolowska, Z., Sokolowski, S., Alekseev, A., Alekseeva, T., 1993. Changes of mineralogical and surface properties of water dispersible clay after acid treatment of soils. Clay Miner. 28, 145–148.

Jozefaciuk, G., Sokolowska, Z., Hajnos, M., Hoffmann, C., Renger, M., 1996. Large effect of leaching of DOC on water adsorption properties of a sandy soil. Geoderma 74, 125–137.

Jozefaciuk, G., Muranyi, A., Szatanik-Kloc, A., Csillag, J., Wlodarczyk, T., 1999. Changes of pore system of a brown forest soil under acid degradation in a laboratory experiment. Pol. J. Soil Sci. XXXII, 23–32.

Lipiec, J., Hatano, R., Slowinska-Jurkiewicz, A., 1998. The fractal dimension of pore distribution patterns in variously-compacted soil. Soil Tillage Res. 47, 61–66.

Neimark, A.V., 1990. Determination of the surface fractal dimensionality from the results of an adsorption experiment. Russ. J. Phys. Chem. 64, 2593–2605.

Newman, A.C.D., 1985. The interaction of water with clay mineral surfaces. In: Newman, A.C.D. (Ed.), Chemistry of Clays and Clay Minerals, Mineralogical Society Monograph no. 6. Longman, London, pp. 237–274.

Oscik, J., 1979. Adsorption. PWN, Warsaw (in Polish).

Pachepsky, Ya.A., Polubesova, T.A., Hajnos, M., Sokolowska, Z., Jozefaciuk, G., 1995a. Fractal parameters of pore surface area as influenced by simulated soil degradation. Soil Sci. Soc. Am. J. 59, 68–75.

Pachepsky, Ya.A., Polubesova, T.A., Hajnos, M., Jozefaciuk, G., Sokolowska, Z., 1995b. Parameters of surface heterogeneity from laboratory experiments on soil degradation. Soil Sci. Soc. Am. J. 59, 410–417.

Petersen, L.W., Moldrup, P., Jacobsen, O.H., Rolston, D.E., 1996. Relation between soil specific area and soil physical and chemical properties. Soil Sci. 161, 9–21.

Pfeifer, P., Obert, M., 1989. Fractals. Basic concepts and terminology. In: Avnir, D. (Ed.), The Fractal Approach to Heterogeneous Chemistry. Wiley, New York, pp. 11–43.

Roquerol, R., Avnir, D., Fairbridge, C.W., Everett, D.H., Haynes, J.H., Pernicone, N., Ramsay, J.D.F., Sing, K.S.W., Unger, K.K., 1994. Recommendations for the characterization of porous solids. Pure Appl. Chem. 66, 1739–1758.

Seelig, B.D., Richardson, J.C., 1994. Sodic soil toposequence related to focused water flow. J. Soil Sci. Soc. Am. 58, 156–163.

Sokolowska, Z., 1989. Role of surface heterogeneity in adsorption processes in soils. Probl. Agrophys. 58, 1–145 (in Polish).

Sokolowska, Z., Jozefaciuk, G., Sokolowski, S., Urumova-Pesheva, A., 1993. Adsorption of water vapor by soils: investigations of the influence of organic matter, iron and aluminum on energetic heterogeneity of soil clays. Clays Clay Miner. 44, 346–352.

Sokolowska, Z., Hajnos, M., Jozefaciuk, G., Kozak, E., Arsova, A., 1995. Profile distribution of water adsorption properties of some representative Bulgarian soils. Soil Sci., Agrochem. Ecol. XXX, 171–173.

Sridharan, A., Venkatappa Rao, G., 1972. Pore size distribution of soils from mercury intrusion porosimetry data. Soil Sci. Soc. Am. Proc. 36, 980–981.

Szendrei, G., 1983. The stability and distribution of clay minerals in Hungarian salt-affected soils. Proceedings 5th Meeting of the European Clay Groups. Charles University, Prague, pp. 471–476.

Toth, T., Kertesz, M., 1996. Application of soil–vegetation correlation to optimal resolution mapping of solonetzic rangeland. Arid Soil Res. Rehabil. 10, 1–12.

Toth, T., Kuti, L., 1999a. Geological factors affecting the salinization of the Nyirolapos Sample Area (Hortobagy, Hungary): I. General geological characterization, calcite concentration and pH values of subsurface layers. Agrokem. Talajtan 48, 431–444 (in Hungarian).

Toth, T., Kuti, L., 1999b. Geological factors affecting the salinization of the Nyirolapos Sample Area (Hortobagy, Hungary): II. Multiple relations and the prediction of surface soil salinity. Agrokem. Talajtan 48, 445–457 (in Hungarian).

Toth, T., Rajkai, K., 1994. Soil and plant correlations in a solonetzic grassland. Soil Sci. 157, 253–262.

Uehara, G., Gillman, G., 1981. The Mineralogy, Chemistry and Physics of Tropical Soils with Variable Charge Clays. Westview Tropical Agriculture Series, 4 Westview, Boulder, CO.

Van Riemsdijk, W.H., Koopal, L.K., De Wit, J.C.M., 1987. Heterogeneity and electrolyte adsorption, intrinsic and electrostatic effects. Neth. J. Soil Sci. 35, 241–257.

Wilczynski, W., Renger, M., Jozefaciuk, G., Hajnos, M., Sokolowska, Z., 1993. Surface area and CEC as related to qualitative and quantitative changes of forest soil organic matter after liming. Z. Pflanzenernaehr. Bodenkd. 156, 235–238.